Mon. Not. R. Astron. Soc. **298,** 42–52 (1998)

A possible theoretical explanation of metallicity gradients in elliptical galaxies

Agostino Martinelli,[1] Francesca Matteucci[2] and Sergio Colafrancesco[3]
[1]*Instituto Astronomico, Via Lancisi 29, Roma, Italy*
[2]*Dipartimento di Astronomia, Università di Trieste and SISSA Institute, via Beirut 2/4, I-34014 Trieste, Italy*
[3]*Osservatorio Astronomico di Roma, Via dell'Osservatorio, I-00040 Monte Porzio, Italy*

Accepted 1998 February 13. Received 1998 February 13; in original form 1997 May 30

ABSTRACT

Models of chemical evolution of elliptical galaxies taking into account different escape velocities at different galactocentric radii are presented. As a consequence of this, the chemical evolution develops differently in different galactic regions; in particular, we find that the galactic wind, powered by supernovae (of Type II and I) starts, under suitable conditions, in the outer regions and successively develops in the central ones. The star formation is assumed to stop after the onset of the galactic wind in each region. The main result found in the present work is that this mechanism is able to reproduce metallicity gradients, namely the gradients in the Mg_2 index, in good agreement with observational data. We also find that in order to honour the constant $[\langle Mg/Fe \rangle]$ ratio with galactocentric distance, as inferred from metallicity indices, a variable initial mass function as a function of galactocentric distance is required. This is only a suggestion, as trends on abundances inferred purely from metallicity indices are still uncertain.

Key words: galaxies: abundances – galaxies: elliptical and lenticular, cD – galaxies: evolution – galaxies: formation.

1 INTRODUCTION

The usefulness of studying elliptical galaxies comes both from the importance for cosmology of knowing their past luminosities and colours and from testing stellar evolution models and theories on supernova progenitors.

Many features shown by elliptical galaxies required, in the past years, theoretical explanations. For example, in order to reproduce the well-known relation between mass and metallicity, Mathews & Baker (1971) and Larson (1974) proposed the existence of galactic winds driven by supernova explosions (note that in such a way they also explained the apparent lack of gas in these systems).

As a result, a great deal of effort has been devoted into studying the detailed chemical evolution of elliptical galaxies (Arimoto & Yoshii 1986, 1987; Matteucci & Tornambè 1987; Brocato et al. 1990; Angeletti & Giannone 1990; Matteucci 1992; Ferrini & Poggianti 1993; Matteucci 1994; Bressan, Chiosi & Fagotto 1994; Matteucci & Gibson 1995; Gibson 1997; Gibson & Matteucci 1997). For example, on the basis of supernova-driven galactic wind models, Matteucci & Tornambè (1987) first analysed the evolution of Mg and Fe in these galaxies and predicted that $[\langle Mg/Fe \rangle]$ should decrease as a function of the galactic mass, at variance with what has been more recently suggested by population synthesis studies (Worthey, Faber & Gonzalez 1992), indicating that $[\langle Mg/Fe \rangle]$ increases with galactic mass in the nuclei of giant ellipticals. Matteucci (1994) pointed out that in order to explain the origin of this relation, one has to assume either that the efficiency of star formation is an increasing function of mass, or that the initial mass function (IMF) should favour more massive stars in more massive galaxies. In the models of Larson (1974), Arimoto & Yoshii (1987) and Matteucci & Tornambè (1987), in fact, the star formation efficiency was either assumed to be constant or to decrease with galactic mass. This last hypothesis was based upon the fact that star formation is mainly determined by cloud–cloud collisions. In this framework the time-scale for star formation (namely the time required to consume all the gas in a galaxy by star formation, and corresponding to the inverse of the star formation efficiency) was assumed to be proportional to the cloud–cloud collision time or to the dynamical free-fall time, with the consequence of decreasing with the galactic mass.

Concerning the other explanation relative to the IMF, the observed variation of the M/L_B ratio in elliptical galaxies as a function of their blue luminosity (Faber & Jackson 1976; Michard 1983; Kormendy & Djorgovski 1989; van den Marel 1991; Bender, Burstein & Faber 1992) seems to argue in favour of a possible variation of the IMF with galactic mass, although other possible explanations cannot be excluded. Renzini & Ciotti (1993), for example, proposed a variable amount and/or concentration of dark matter as a function of luminous mass; Zepf & Silk (1996) analysed the hypothesis that star formation includes a phase in which star formation is restricted to massive stars, with the bias towards high-mass stars increasing with galactic mass.

The evidence for a mass–metallicity relation in ellipticals comes not only from changes in colours with galactic luminosity (Faber 1972), but also from the linear relationship existing between the Mg_2 index as defined by Faber et al. (1985) and the internal velocity dispersion σ (Dressler et al. 1987; Bender, Burstein & Faber 1993). It is generally assumed, in fact, that these colour and metallicity index changes indicate variations in metallicity.

Ziegler (1997) found that determining the Mg_b–σ (Mg_b is another metallicity indicator, always referring to Mg, as defined in Faber et al. 1985) relations at various redshifts is a powerful and robust method to measure the evolution of elliptical galaxies. In his work he points out two conclusions: first, the stellar population of elliptical cluster galaxies evolves passively between $z = 0.4$ and today, and secondly, the epoch of formation of the stars that form the present-day ellipticals occurred at high redshifts ($z > 2$ and the most luminous objects might have formed even at $z > 4$).

Another important aspect of the Mg_b–σ relation is its small scatter. This is usually interpreted as an indication that the process of galaxy formation was short (see Renzini 1995).

Metallicity gradients are also well-known characteristics of elliptical galaxies (Carollo, Danziger & Buson 1993; Davies, Sadler & Peletier 1993). The best evidence comes from the spectroscopic measurements of absorption lines in ellipticals (Faber 1977; Burnstein et al. 1984; Faber et al. 1985; Peletier 1989). Typically, the Mg_b and Fe absorption-line strengths are stronger in high-mass galaxies. In individual galaxies they generally decrease outwards from the centre. The colours behave similarly, being redder in high-mass galaxies and changing from red to blue outwards. Therefore, both the colour and line-strength changes indicate consistently that these gradients are very likely caused by variations in metallicity. However, the mechanism by which these metallicity variations could have arisen is still unclear. The models proposed are based on the processes developed during galaxy formation. Larson (1974) and Carlberg (1984) showed that elliptical galaxies, which form by dissipative collapse of a primordial gas cloud, should have an increasing metallicity with decreasing radius. The idea is that the stars begin to form everywhere during the collapse and remain in orbit with a little inward motion, whereas the gas falls towards the centre and is enriched by the evolving stars. In this way, the stars that form at the galaxy centre are more metal-enriched than those formed in the external regions. These models produce galaxies with very steep metallicity gradients: a factor of 10 reduction in metallicity for a factor of 10 increase in radius. Carlberg's models include a pressure term associated with the energy input from supernovae during the collapse. This decreases the size of abundance gradients in the final galaxies to a factor of 3 over each decade in radius.

Franx & Illingworth (1990) found that, for their sample of 17 galaxies, the local $(B - R)$ $(U - R)$ colours are functions of the local escape velocity v_{esc} for all of the galaxies. This result was confirmed later by Davies et al. (1993) and Carollo & Danziger (1994) using a more direct indicator of metallicity (Mg_2) than colours and a more appropriate calculation of v_{esc} for each galaxy. This relation suggests that metallicity gradients could have arisen because of the different times of occurrence of galactic winds in different galactic regions. In fact, the galactic wind starts when the energy injected in the interstellar medium (ISM) by supernovae (of both Type I and II) becomes equal to the binding energy of the gas (Larson 1974). Moreover, it is reasonable to think that when the galactic wind starts the SFR breaks down. Hence, in the regions where v_{esc} is low (i.e. where the local potential is shallow), the galactic wind will develop earlier and the gas is less processed than in the regions where v_{esc} is higher, and the potential well in the external regions is lower than in the internal regions.

The aim of this paper is to discuss the formation of abundance gradients in elliptical galaxies. The model suggested here to explain metallicity gradients does not follow in detail the processes occurring during galaxy formation such as collapse or merging, and it starts with the total galactic mass already present at the beginning. This is a good assumption for elliptical galaxies because they must have formed in a reasonably short time-scale (Matteucci 1994; Renzini 1995; Ziegler 1997), as already discussed. Recently, Kauffmann & Charlot (1998) have discussed the formation of ellipticals by merging of spirals in the context of a hierarchical clustering scenario. This mechanism would imply a much longer process than that adopted here and it certainly cannot explain the high [⟨Mg/Fe⟩] ratios found in the nuclei of ellipticals. Moreover, recently Prochaska & Wolfe (1997) showed that the Kauffmann (1996) model is inconsistent with the damped Lyman α data.

The results we present here are obtained using a code of chemical evolution (Matteucci & Gibson 1995, hereafter MG) modified in order to take into account the different evolution of each galactic region.

This paper is organized into four sections. Section 2 concerns the new theoretical prescriptions with respect to MG; the theoretical results are discussed and compared with observations in Section 3, where models of a galaxy with a mass of 10^{11} $M_\odot$ are discussed for illustrative purposes. Finally, some conclusions and remarks are made in Section 4.

2 THEORETICAL PRESCRIPTIONS

2.1 The chemical evolution model

In the following, we consider elliptical galaxies to have spherical symmetry. We assume that at the initial time ($t = 0$) these systems consist only of primordial gas, and the star formation starts at the same time in all galactic regions.

The galaxy is partitioned in zones having the shape of spherical shells. The basic equations to calculate the chemical evolution in each zone are the same as in MG and, for this reason, they will not be repeated here. We will only remind the reader that the model belongs to the category of supernova-driven wind models and follows the evolution in space and time of the abundances of several chemical elements (H, D, ^{3}He, ^{4}He, C, N, O, Ne, Mg, Si, Fe and others). The stellar lifetimes are taken into account and the rates of supernovae of Type II and I are computed in detail. In particular, for the rate of Type Ia supernovae, which are assumed to originate in white dwarfs in binary systems, we adopt the original formulation described in Matteucci & Greggio (1986) and Matteucci & Tornambè (1987).

2.2 Stellar birth-rate function

The stellar birth-rate function is generally separated into two independent functions:

$$B(m, t) = \psi(t)\phi(m). \quad (1)$$

Following MG, $\psi(t)$ is given by

$$\psi(t) = \nu\rho_{gas}(t), \quad (2)$$

where $\rho_{gas}(t)$ is the volume gas density in the region of interest at the time t. The parameter ν represents the star formation efficiency and is taken from Arimoto & Yoshii (1986): $\nu = 8.6[M_{gas}(0)/10^{12}\ M_\odot]^{-0.115}$ (Gyr^{-1}), and is assumed to be constant with radius.

The IMF is generally expressed as a power law and here we consider

$$\phi(m) \propto m^{-x}, \tag{3}$$

normalized to unity in the mass range $0.1 \leq M/\mathrm{M}_{\odot} \leq 100$. We have explored three different cases:

(i) $x = 0.95$ for all regions of the galaxy;
(ii) $x = 1.35$ for all regions of the galaxy;
(iii) x variable and in particular increasing with radius.

2.3 Stellar yields

We adopted the same stellar yields as in MG in order to be able to compare our results with theirs. In particular we assumed the following.

(i) For massive stars and supernovae II ($M > 8$ $\mathrm{M}_{\odot}$) the yields of Woosley (1987) are adopted.

(ii) For low- and intermediate-mass stars ($0.8 \leq M/\mathrm{M}_{\odot} \leq 8$) we assume the yields of Renzini & Voli (1981).

(iii) For Type Ia supernovae the yields of Thielemann, Nomoto & Hashimoto (1993) for their model W7 are used. The stellar lifetimes are the same as adopted by Matteucci & Padovani (1993), namely

for $M > 6.6$ $\mathrm{M}_{\odot}$

$$\tau_m = 1.2m^{-1.85} + 0.003 \text{ Gyr}, \tag{4}$$

and for $M \leq 6.6$ $\mathrm{M}_{\odot}$

$$\tau_m = 10^{1.338-\sqrt{1.790-0.2232\cdot(7.764-\log m)}} - 9 \text{ Gyr}. \tag{5}$$

For the details of calculation of the Type Ia SN rate we address the reader to MG. We will remind the reader here only that the fraction of binary systems is a function of the assumed IMF as described in MG.

2.4 Galactic wind

Galactic winds in ellipticals were originally introduced to reproduce the well-known mass–metallicity relation in these systems and to explain the apparent lack of gas (Larson 1974). However, besides this, galactic winds are the natural consequence of a phase of intense star formation. The existence of a galactic wind, in fact, is strictly related to the energetics of the interstellar medium compared with the potential energy of the gas. The time at which a galactic wind occurs is a fundamental parameter for the chemical evolution of a galaxy region. The condition that should be satisfied for the gas to be ejected from a given region is expressed by the following condition (Larson 1974):

$$E^i_{\mathrm{th_{SN}}}(t_{\mathrm{GW}}) = E^i_{\mathrm{Bgas}}(t_{\mathrm{GW}}), \tag{6}$$

where the index i indicates the particular region under consideration.

The condition requires that the thermal energy of the gas in a given region, resulting from supernova explosions in that region, must exceed the binding energy of the gas. For both quantities in equation (6) we used new theoretical prescriptions with respect to previous works. These prescriptions will be described in the next sections.

2.5 The potential energy of the gas, E_{Bgas}

We define E_{Bgas} as the energy necessary to carry the gas of a given galactic region outside the galaxy.

With reference to a spherical shell region of thickness ΔR_i and internal and external radii R_i and $R_{i+1} = R_i + \Delta R_i$ respectively, the energy E_{Bgas} can be written as follows:

$$E^i_{\mathrm{Bgas}} = \int_{R_i}^{R_i+\Delta R_i} \mathrm{d}L(r), \tag{7}$$

where $\mathrm{d}L(r)$ is the energy required to carry out a quantity $\mathrm{d}m = 4\pi r^2 f_{\mathrm{g}}(r,t)\mathrm{d}r$ of gas. Here $f_{\mathrm{g}}(r,t)$ is the density function of the gas, depending on the distance r from the galactic centre and on the galactic age t. Therefore, we have for $\mathrm{d}L(r)$

$$\mathrm{d}L(r) = \int_r^{\infty} \mathrm{d}r' f(r') \tag{8}$$

where $f(r')$ is the force between $\mathrm{d}m$ and the total mass (dark and luminous) within r', which reads as

$$f(r') = \frac{GM(r')\mathrm{d}m}{r'^2}. \tag{9}$$

The range of integration in (8) can be reasonably limited to an upper effective radius, because we only require that the gas leaves the galaxy. For this reason we replace ∞ with $(1+a)R_{\mathrm{e}}$, where R_{e} is the effective galaxy radius and $a \geq 0$. As a consequence of this, $\mathrm{d}L(r) = \int_r^{(1+a)R_{\mathrm{e}}} \mathrm{d}r' f(r')$. In practice, we have analysed two cases: (i) $a = 0.5$ which corresponds to the case in which the gas is carried out to $1.5R_{\mathrm{e}}$, and (ii) $a = \infty$ which corresponds to the case in which the gas is carried out to infinity. The influence of a finite value of a will be discussed in Section 3.

The total mass at radius r', $M(r')$, is given by

$$M(r') = M_{\mathrm{Dark}}(r') + M_{\mathrm{Lum}}(r'), \tag{10}$$

where the luminous mass can be written as the sum of the gaseous and stellar components:

$$M_{\mathrm{Lum}}(r') = M_{\mathrm{gas}}(r') + M_*(r'). \tag{11}$$

Assuming the same distribution for the two components, we have

$$M_{\mathrm{gas}}(r') = \rho_{\mathrm{g}} F_1(r'); \tag{12}$$

$$M_*(r') = \rho_* F_1(r'); \tag{13}$$

$$F_1(r') = 4\pi \int_0^{r'} \mathrm{d}s f_1(s) s^2. \tag{14}$$

The quantities appearing in equations (12), (13) and (14) can be determined on the basis of prescriptions available in the literature. Namely, we have for $F_1(r)$ (Jaffe 1983)

$$F_1(r) \propto \frac{r_+}{1 + r/_+}, \tag{15}$$

with $r_+ = R_{\mathrm{e}}/0.763$, and for the dark matter distribution we have (Bertin, Saglia & Stiavelli 1992)

$$M_{\mathrm{Dark}}(r) = \frac{2M_{\mathrm{Dark}}}{\pi}\left[\arctan(r/r_0) - \frac{r/r_0}{1+(r/r_0)^2}\right], \tag{16}$$

with $r_0 = 0.45R_{\mathrm{Dark}}$. In the following, three different cases for the distribution of dark matter will be analysed:

(i) $M_{\mathrm{Dark}} = 0$,
(ii) $M_{\mathrm{Dark}} = 10M_{\mathrm{Lum}}$ and $R_{\mathrm{Dark}} = 10R_{\mathrm{e}}$, and
(iii) $M_{\mathrm{Dark}} = 10M_{\mathrm{Lum}}$ and $R_{\mathrm{Dark}} = R_{\mathrm{e}}$.

These cases have been chosen because they represent extreme cases going from no dark matter (except the stellar remnants) to an amount of dark matter 10 times the luminous one, either distributed in a diffuse halo or tracing the luminous material. All the other possibilities will therefore be intermediate between these cases.

In the case $a = \infty$, $R_i = 0$, $R_{i+1} = R_e$ (i.e. one-zone model), considering luminous matter uniformly distributed and in the absence of dark matter, equation (7) gives

$$E_{\rm Bgas} = \frac{3}{5}\frac{G}{R_e} M_{\rm gas}(2M_* + M_{\rm gas}). \quad (17)$$

2.6 The thermal energy of the gas caused by supernovae, $E_{\rm th_{SN}}$

The total thermal energy in the gas at time t is

$$E_{\rm th_{SN}}(t) = \int_0^t \epsilon_{\rm th_{SN}}(t - t')R_{\rm SN}(t')\mathrm{d}t', \quad (18)$$

where $R_{\rm SN}(t)$ is the SN rate and $\epsilon_{\rm th_{SN}}(t_{\rm SN})$ is the thermal energy content inside a supernova remnant of both types, with $t_{\rm SN} = t - t'$. $\epsilon_{\rm th_{SN}}(t_{\rm SN})$ evolves, according to Cox (1972), in the following way:

$$\epsilon_{\rm th_{SN}}(t_{\rm SN}) = 7.2 \times 10^{50}\epsilon_0 \ \mathrm{erg} \quad (19)$$

for $0 \leq t_{\rm SN} < t_c$, and

$$\epsilon_{\rm th_{SN}}(t_{\rm SN}) = 2.2 \times 10^{50}\epsilon_0 (t_{\rm SN}/t_c)^{-0.62} \ \mathrm{erg} \quad (20)$$

for $t_{\rm SN} \geq t_c$,

where ϵ_0 is the initial blast wave energy in units of 10^{51} erg, $t_{\rm SN}$ is the time elapsed since the supernova explosion, t_c is the cooling time of a supernova remnant, namely

$$t_c = 5.710^4 \epsilon_0^{4/17} n_0^{-9/17} \ \mathrm{yr}, \quad (21)$$

and $n_0(t) = \rho(t)/\langle m \rangle$ is the average number density of the ISM. Gibson (1997) adopted a more sophisticated treatment for the calculation of $E_{\rm th_{SN}}$, based on calculations by Cioffi, McKee & Bertschinger (1988). However, given the uncertainties present in this kind of calculations we have decided to adopt the old formulation, common to most of the previous papers on the chemical evolution of ellipticals. We did not consider the energy injected into the ISM by stellar winds, because for massive galaxies it is negligible, as shown by Gibson (1994).

3 RESULTS AND CONCLUSIONS

3.1 Model parameters

We have calculated several chemical evolution models by varying the amount and distribution of dark matter as well as the parameter a and we have also considered either the case of a constant IMF in all the regions of the galaxy or the case of an IMF varying with the galactocentric distance. In Table 1 we show the choice of the parameters for all the models referring to the case with constant IMF. In particular, in this table we indicate the amount of dark matter (column two) and the distribution of dark matter (column three). Finally, in column four we show the adopted value of the parameter a. We have used two different values for the IMF slope in the models, with an IMF constant in radius: $x = 0.95$ and $x = 1.35$ (Salpeter 1955).

Table 1. Models considered. The parameter a, in the fourth column, fixes the distance at which the gas is carried out of the galaxy, namely $(1 + a)R_e$.

MODEL	$\frac{M_D}{M_L}$	$\frac{R_D}{R_L}$	a
A1	0	/	∞
A2	0	/	0.5
B1	10	10	∞
B2	10	10	0.5
C1	10	1	∞
C2	10	1	0.5

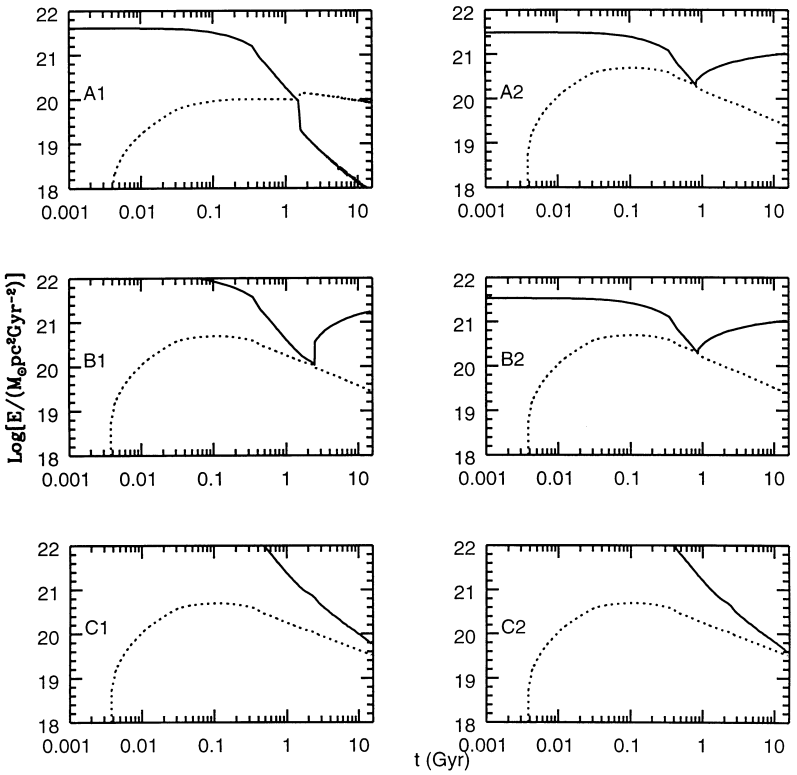

Figure 1. $E_{\rm Bgas}$ (solid line) and $E_{\rm th_{SN}}$ (dotted line) for the six models in the case of one zone.

In the framework of the models with a variable IMF we considered only one case in which all the parameters are the same as in the B2 model, except for the IMF slope. We will refer to this last case as model IV, where the IMF slope varies from $x = 0.95$ in the internal regions to $x = 1.21$ in the external ones. This choice is made in order to have [⟨Mg/Fe⟩] constant in radius, as it will be shown. Observational results seem, in fact, to indicate that [⟨Mg/Fe⟩] as a function of the galactocentric distance is roughly constant, at variance with what happens for the central [⟨Mg/Fe⟩] as a function of galactic mass (Worthey et al. 1992; Carollo et al. 1993; Davies et al. 1993). However, there is a warning here, namely the trends on real abundances inferred from metallicity indices may be deceiving as recently suggested by Tantalo, Bressan & Chiosi (1998). In all cases the values of t_{GW}, and the mass-averaged abundances of Fe and Mg, namely [⟨Fe/H⟩] and [⟨Mg/Fe⟩], will be calculated for a galaxy of 10^{11} $M_\odot$ of luminous mass and $R_e = 3$ kpc.

3.2 Galactic winds

The results concerning galactic winds are summarized in Fig. 1 and Tables 2–14. Fig. 1 shows the behaviour of E_{Bgas} (solid line) and $E_{th_{SN}}$ (dotted line) for the six one-zone models. The occurrence of galactic winds is affected by the presence of dark matter, depending on the value of a. The value of a sets the distance at which the gas is ejected. Small values of a imply the presence of gas near the galaxy whereas large values of a imply that the gas is carried outside the gravitational field of the galaxy. This formulation allows us to study different cases, unlike the model of Matteucci (1992) which corresponded only to the case of small a. Although a dynamical model would be necessary to assess whether the gas mass is definitely lost from the galaxy or whether it remains around it, different values of the parameter a may influence the chemical enrichment of the intracluster medium (ICM), in the sense that large values of a will predict a higher contribution from the galaxies to the ICM. To be more precise, the influence of dark matter is very strong for all values of a when it is distributed like the luminous matter

Table 2. Model A1 with the IMF slope (x) constant in radius and equal to 0.95.

$Log(\frac{R}{R_e})$	t_{GW}	$[<\frac{Fe}{H}>]$	Mg_2	$[<\frac{Mg}{Fe}>]$
–2.233	/	0.68	0.400	0.15
–1.929	/	0.68	0.400	0.15
–1.385	13.5	0.68	0.400	0.15
–0.963	5.0	0.65	0.394	0.17
–0.824	3.6	0.63	0.391	0.18
–0.602	2.5	0.59	0.385	0.20
–0.424	1.5	0.55	0.378	0.22
–0.279	1.1	0.52	0.373	0.24
–0.137	0.82	0.48	0.366	0.25
0.000	0.62	0.43	0.357	0.27

Table 3. Model A2 with $x = 0.95$.

$Log(\frac{R}{R_e})$	t_{GW}	$[<\frac{Fe}{H}>]$	Mg_2	$[<\frac{Mg}{Fe}>]$
–2.233	/	0.68	0.400	0.15
–1.929	/	0.68	0.400	0.15
–1.385	11.8	0.67	0.400	0.15
–0.963	4.3	0.64	0.393	0.17
–0.824	3.1	0.62	0.389	0.18
–0.602	1.7	0.56	0.380	0.22
–0.424	1.1	0.53	0.374	0.24
–0.279	0.86	0.49	0.367	0.25
–0.137	0.58	0.42	0.355	0.27
0.000	0.40	0.31	0.336	0.29

Table 4. Model B1 with $x = 0.95$.

$Log(\frac{R}{R_e})$	t_{GW}	$[<\frac{Fe}{H}>]$	Mg_2	$[<\frac{Mg}{Fe}>]$
–2.233	/	0.68	0.400	0.15
–1.929	/	0.68	0.400	0.15
–1.385	/	0.68	0.400	0.15
–0.963	9.4	0.67	0.398	0.15
–0.824	7.0	0.66	0.397	0.16
–0.602	4.5	0.64	0.393	0.17
–0.424	3.0	0.62	0.389	0.18
–0.279	2.4	0.59	0.385	0.20
–0.137	1.7	0.56	0.380	0.22
0.000	1.3	0.54	0.376	0.23

Table 5. Model B2 with $x = 0.95$.

$Log(\frac{R}{R_e})$	t_{GW}	$[<\frac{Fe}{H}>]$	Mg_2	$[<\frac{Mg}{Fe}>]$
–2.233	/	0.68	0.400	0.15
–1.929	/	0.68	0.400	0.15
–1.385	11.9	0.68	0.399	0.15
–0.963	4.1	0.64	0.393	0.17
–0.824	3.0	0.62	0.389	0.18
–0.602	1.8	0.57	0.381	0.21
–0.424	1.2	0.53	0.375	0.23
–0.279	0.87	0.50	0.368	0.25
–0.137	0.59	0.43	0.358	0.27
0.000	0.35	0.31	0.336	0.29

Table 6. Model C1 with $x = 0.95$.

$Log(\frac{R}{R_e})$	t_{GW}	$[<\frac{Fe}{H}>]$	Mg_2	$[<\frac{Mg}{Fe}>]$
–2.233	/	0.68	0.400	0.15
–1.929	/	0.68	0.400	0.15
–1.385	/	0.68	0.400	0.15
–0.963	/	0.68	0.400	0.15
–0.824	/	0.68	0.400	0.15
–0.602	/	0.68	0.400	0.15
–0.424	/	0.68	0.400	0.15
–0.279	9.9	0.67	0.398	0.15
–0.137	5.9	0.65	0.396	0.16
0.000	3.8	0.63	0.392	0.18

Table 7. Model C2 with $x = 0.95$.

$Log(\frac{R}{R_e})$	t_{GW}	$[<\frac{Fe}{H}>]$	Mg_2	$[<\frac{Mg}{Fe}>]$
−2.233	/	0.68	0.400	0.15
−1.929	/	0.68	0.400	0.15
−1.385	/	0.68	0.400	0.15
−0.963	/	0.68	0.400	0.15
−0.824	/	0.68	0.400	0.15
−0.602	/	0.68	0.400	0.15
−0.424	9.5	0.67	0.398	0.15
−0.279	5.0	0.65	0.394	0.17
−0.137	2.7	0.61	0.388	0.19
0.000	1.4	0.54	0.376	0.23

Table 8. Model A1 with $x = 1.35$.

$Log(\frac{R}{R_e})$	t_{GW}	$[<\frac{Fe}{H}>]$	Mg_2	$[<\frac{Mg}{Fe}>]$
−2.233	/	0.55	0.378	−0.32
−1.929	/	0.55	0.378	−0.32
−1.385	/	0.55	0.378	−0.32
−0.963	5.3	0.50	0.369	−0.29
−0.824	3.6	0.46	0.362	−0.27
−0.602	2.0	0.35	0.343	−0.19
−0.424	1.26	0.26	0.329	−0.13
−0.279	0.90	0.20	0.318	−0.084
−0.137	0.72	0.14	0.308	−0.044
0.000	0.56	0.071	0.296	0.0030

Table 9. Model A2 with $x = 1.35$.

$Log(\frac{R}{R_e})$	t_{GW}	$[<\frac{Fe}{H}>]$	Mg_2	$[<\frac{Mg}{Fe}>]$
−2.233	/	0.55	0.378	−0.32
−1.929	/	0.55	0.378	−0.32
−1.385	14.3	0.55	0.378	−0.32
−0.963	4.3	0.48	0.366	−0.28
−0.824	2.9	0.43	0.357	−0.25
−0.602	1.6	0.31	0.336	−0.16
−0.424	0.96	0.21	0.320	−0.094
−0.279	0.72	0.14	0.308	−0.044
−0.137	0.56	0.071	0.296	0.0030
0.000	0.43	0.025	0.288	0.030

Table 10. Model B1 with $x = 1.35$.

$Log(\frac{R}{R_e})$	t_{GW}	$[<\frac{Fe}{H}>]$	Mg_2	$[<\frac{Mg}{Fe}>]$
−2.233	/	0.55	0.378	−0.32
−1.929	/	0.55	0.378	−0.32
−1.385	/	0.55	0.378	−0.32
−0.963	11.8	0.54	0.377	−0.32
−0.824	7.4	0.52	0.373	−0.31
−0.602	4.4	0.49	0.367	−0.29
−0.424	3.0	0.43	0.357	−0.25
−0.279	2.3	0.36	0.346	−0.20
−0.137	1.6	0.31	0.336	−0.16
0.000	1.1	0.25	0.327	−0.12

Table 11. Model B2 with $x = 1.35$.

$Log(\frac{R}{R_e})$	t_{GW}	$[<\frac{Fe}{H}>]$	Mg_2	$[<\frac{Mg}{Fe}>]$
−2.233	/	0.55	0.378	−0.32
−1.929	/	0.55	0.378	−0.32
−1.385	14.3	0.55	0.378	−0.32
−0.963	4.5	0.48	0.366	−0.28
−0.824	3.1	0.44	0.358	−0.25
−0.602	1.8	0.32	0.338	−0.17
−0.424	1.0	0.23	0.323	−0.10
−0.279	0.78	0.17	0.312	−0.060
−0.137	0.56	0.071	0.296	0.0030
0.000	0.43	0.025	0.288	0.030

Table 12. Model C1 with $x = 1.35$.

$Log(\frac{R}{R_e})$	t_{GW}	$[<\frac{Fe}{H}>]$	Mg_2	$[<\frac{Mg}{Fe}>]$
−2.233	/	0.55	0.378	−0.32
−1.929	/	0.55	0.378	−0.32
−1.385	/	0.55	0.378	−0.32
−0.963	/	0.55	0.378	−0.32
−0.824	/	0.55	0.378	−0.32
−0.602	/	0.55	0.378	−0.32
−0.424	/	0.55	0.378	−0.32
−0.279	11.9	0.54	0.377	−0.32
−0.137	7.1	0.52	0.373	−0.31
0.000	3.9	0.47	0.364	−0.27

(models C1 and C2). However, when dark matter is distributed in a diffuse halo, its effect is relevant only for high values of a (B1): in fact, in this case we are considering the potential energy of the gas as the energy to carry the gas out of the halo. On the other hand, a diffuse halo of dark matter does not affect the occurrence of the galactic wind if we use small values of a (B2). This last result is in agreement with Matteucci (1992): she defined the potential energy as the energy to carry the gas out of the galaxy, namely to the distance $R_e(a = 0)$.

Tables 2–14 give the values of t_{GW} for the models in the case of 10 zones with IMF slope equal to 0.95 (Tables 2–7), 1.35 (Tables 8–13) and variable (Table 14) (the zone thickness is obtained directly from data observations by Davies et al. 1993).

From these tables we note that galactic winds are present only in a small number of outer regions for models C. Namely, the wind occurs only for $r > 1.5$ kpc and $r > 1.0$ kpc for models C1 and C2 respectively. Consequently, models C predict that much smaller gas masses are ejected from the galaxy and that masses forming the hot coronae are smaller than those estimated from the X-ray emission (Forman, Jones & Tucker 1985; Canizares, Fabbiano & Trinchieri 1987). Such galaxies should also show active star formation at intermediate redshifts ($z < 1$), which seems not to be the case for normal ellipticals (Matteucci 1994; Renzini 1995; Ziegler 1997). Therefore, we are tempted to reject the hypothesis of dark matter distributed like luminous matter (as already pointed out by Matteucci 1992).

With regards to models A1, A2 and B2, we note that they are very similar to those in the case of one zone. For these models, galactic winds occur in the internal regions after several Gyr since galaxy formation (note that in the most internal region, with $r < 30$ pc, the wind never occurs), while in the most external regions they occur before 1.0 Gyr from the epoch of galaxy formation.

This time spread of the galactic wind occurrence with the galactocentric distance has very important consequences for the chemical evolution in clusters of galaxies. Previous one-zone models, in fact, including massive, diffuse, dark matter components (B2 models), undergo only a global 'impulsive' ejection of their ISMs at t_{GW} (the same result was pointed out by MG), also for different prescriptions of the IMF and SFR. Therefore, these one-zone models do not predict any chemical evolution in the ICM after nearly 1 Gyr from galaxy formation, when galactic winds have already occurred in all the galaxies. On the other hand, the multi-zone models predict chemical evolution in the ICM also at the present time because, even if there is only one global 'impulsive' ejection of gas in all the regions of the galaxy, the most internal regions eject the processed gas very late. Another consequence, which we will see in the next paragraphs, is the predicted behaviour of $[\langle Mg/Fe \rangle]$ in stars, which tends to increase with increasing radius, unless a variable IMF is assumed. This could be a potential problem because the galactic wind occurring late in the most internal regions of ellipticals might mean active star formation at small redshifts, which is not observed in these galaxies. However, as is shown in Fig. 2, the present time SN II rate (and therefore the SFR) predicted by our best model IV in the most internal regions (< 150 pc) is negligible (about 0.01 times the SN rate of our Galaxy). This is a

Table 13. Model C2 with $x = 1.35$.

$Log(\frac{R}{R_e})$	t_{GW}	$[<\frac{Fe}{H}>]$	Mg_2	$[<\frac{Mg}{Fe}>]$
−2.233	/	0.55	0.378	−0.32
−1.929	/	0.55	0.378	−0.32
−1.385	/	0.55	0.378	−0.32
−0.963	/	0.55	0.378	−0.32
−0.824	/	0.55	0.378	−0.32
−0.602	/	0.55	0.378	−0.32
−0.424	11.3	0.54	0.376	−0.32
−0.279	5.2	0.50	0.369	−0.29
−0.137	2.5	0.40	0.352	−0.22
0.000	1.1	0.25	0.327	−0.12

Table 14. Results related to 10-zone IV model. The IMF is radius-dependent in order to have $[\langle Mg/Fe \rangle]$ constant (= 0.15).

$Log(\frac{R}{R_e})$	t_{GW}	$[<\frac{Fe}{H}>]$	Mg_2	x
−2.233	/	0.68	0.400	0.95
−1.929	/	0.68	0.400	0.95
−1.385	12.3	0.68	0.400	0.95
−0.963	4.4	0.64	0.393	0.97
−0.824	3.1	0.61	0.389	0.98
−0.602	1.8	0.54	0.376	1.02
−0.424	1.2	0.47	0.364	1.05
−0.279	0.80	0.42	0.350	1.09
−0.137	0.58	0.39	0.333	1.13
0.000	0.48	0.17	0.312	1.21

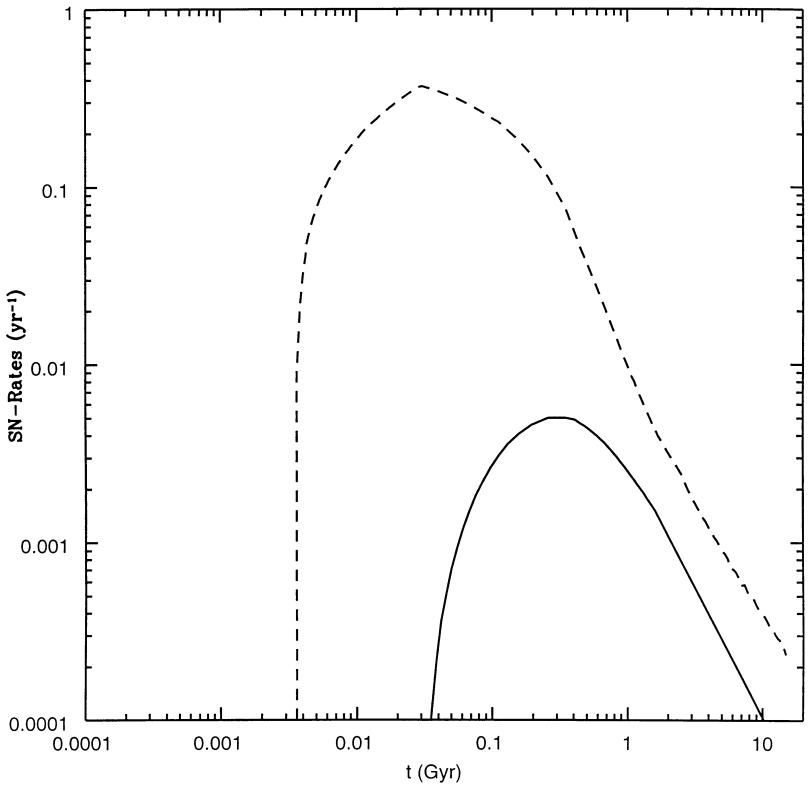

Figure 2. The Type II (dashed line) and Ia (continuous line) SN rates, expressed in units of SNe yr^{-1}, as a function of time (expressed in Gyr), as predicted by model IV. The figure refers to the most internal regions, i.e. the only regions where the SFR is active after 3 Gyr.

result of the fact that the gas is consumed by star formation much before the galactic wind occurs. We do not show the SN rates for our model B2 ($x = 0.95$) because they are very similar to the results of model IV.

3.3 Metallicity in stars

According to the model of chemical evolution used, each region of elliptical galaxies has a composite stellar population containing stars of different ages and metallicities. This is, of course, true also in reality because the process of star formation is not instantaneous. In order to compare theoretical results with the metallicity abundances indicated by the observed indices, we should first calculate the average iron and magnesium abundances in the composite stellar populations. The mass-averaged metallicity of a composite stellar population is defined following Pagel & Patchett (1975) as

$$\langle Z\rangle_M = \frac{1}{S_1}\int_0^{S_1} Z(S)\mathrm{d}S \qquad (22)$$

where the subscript 1 indicates a specific time t_1, which in our case is the present time, assumed to be 15 Gyr, and S is the total mass of stars ever born. According to the definition above we can calculate the average iron and magnesium abundances, because the model provides the functions $X_{\rm Fe}(S)$ and $X_{\rm Mg}(S)$. However, it should be noted that, although the mass-averaged metallicity represents the real average metallicity of the composite stellar population, what should be compared with the metallicities deduced from observations is the luminosity-averaged metallicity. In fact, the metallicity indices, measured from integrated spectra, represent the metallicity of the stellar population that predominates in the visual light. The transformation from metallicity indices to real abundances should then be performed through either theoretical or empirical calibrations relating metallicity indices to real abundances. Galactic chemical evolution models (Arimoto & Yoshii 1987; Matteucci & Tornambè 1987) have shown that the two averaged metallicities are different, because metal-poor giants tend to predominate in the visual luminosity so that, in general, the luminosity-averaged metallicity is smaller than the mass-averaged one. However, the difference is negligible for galaxies with mass $M \geq 10^{11}$ $\mathrm{M}_\odot$, which is the case we discuss here, and we are interested mainly in studying metallicity gradients, which are clearly not affected by the absolute value of the metallicity.

The results concerning $[\langle\mathrm{Fe/H}\rangle] = \log\langle\mathrm{Fe/H}\rangle - \log(\mathrm{Fe/H})_\odot$ and the indices are summarized in the third and fourth columns of Tables 2–14. In these same tables we report the logarithm of (R/R_e) (column one) and the time for the onset of galactic winds expressed in Gyr (column two). In all the tables except Table 14, column 5 shows the $[\langle\mathrm{Mg/Fe}\rangle]$ ratio. In Table 14 we show instead in column five the adopted values for the IMF slope as a function of the galactocentric distance. In this model $[\langle\mathrm{Mg/Fe}\rangle]$ is constant as a function of the galactocentric distance ($[\langle\mathrm{Mg/Fe}\rangle] = 0.15$), because we selected the IMF slope in order to achieve this result. The value of $[\langle\mathrm{Fe/H}\rangle]$ (column 3) is transformed into Mg_2 (column 4) by using the calibration of Worthey (1994) corresponding to an age of the dominant stellar population of 17 Gyr and $[\langle\mathrm{Mg/Fe}\rangle] = 0$.

In models A2 and B2 with $x = 1.35$ we obtain for $[\langle\mathrm{Fe/H}\rangle]$ values of 0.55 and 0.025 respectively in the central and external regions. Correspondingly we obtain a gradient of $\Delta[\langle\mathrm{Fe/H}\rangle]/(\Delta\log r) = -0.27$ dex. We also tried to use other calibrations available in the literature (Buzzoni, Gariboldi & Mantegazza 1992; Mould 1978; Barbuy 1994) and we found differences in the absolute values of Mg_2 up to $\sim$0.1 dex.

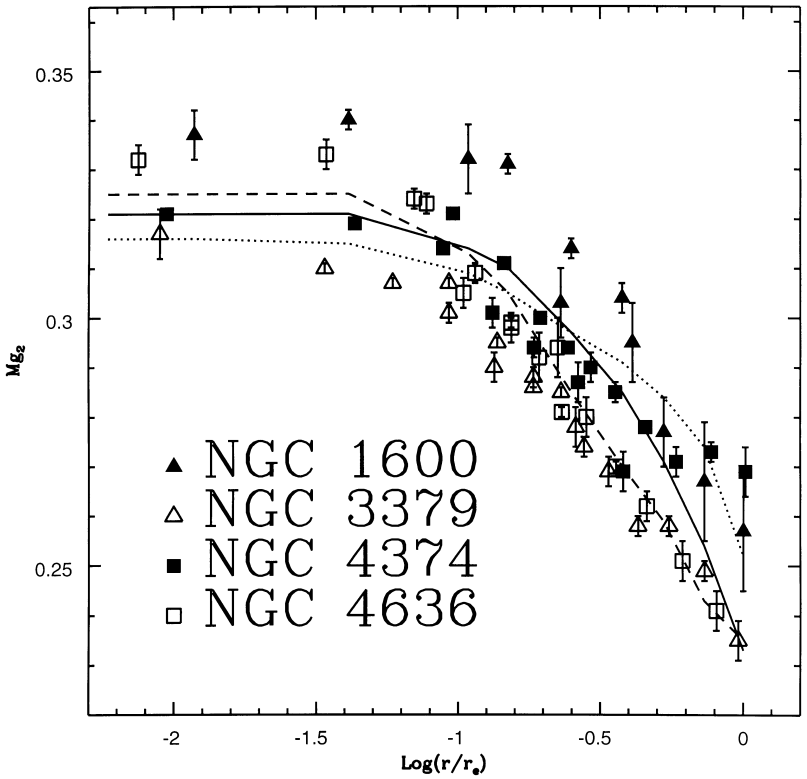

Figure 3. Predicted and observed gradients of the metallicity index Mg_2. The data refer to galaxies in the sample observed by Davies et al. (1993). The continuous line refers to model IV, the dashed line to model B2 ($x = 1.35$) and the dotted line to model B2 ($x = 0.95$). The error bars in the data are also shown. The calibration adopted to transform $[\langle\mathrm{Fe/H}\rangle]$ into Mg_2 is that of Worthey (1994) relative to an age of 17 Gyr.

In Fig. 3 the predicted values of Mg_2 versus radial distance from the galactic centre are shown together with data from Davies et al. (1993). The data refer to galaxies of the same size as our typical galaxy. In the figure the solid line represents the predictions of model IV, whereas dotted and dashed lines represent the predictions of model B2 with $x = 0.95$ and 1.35, respectively. Theoretical values are systematically larger than observational data. This fact may be caused by the uncertainties related to the metallicity calibration and the stellar yields. On the basis of the previous remark it is interesting to note that a better matching between theoretical and experimental data can be simply obtained by shifting the theoretical curves by a suitable amount. The shifts we applied are -0.079 dex for model IV, -0.084 for model B2 (0.95) and -0.05 for model B2 (1.35). These shifts are well inside the differences we obtained by changing calibrations and/or by using models of different ages as shown in Fig. 4, where the predictions of our best model (model IV) are transformed according to the calibrations of Worthey (1994) for different ages of the dominant stellar populations and $[\langle Mg/Fe\rangle] = 0$. In any case, we do not think that is very important to fit the absolute values of Mg_2, given the still existing uncertainties, but rather it is more meaningful to fit the gradient itself, and our models produce a very good fit. In particular, the model with $x = 1.35$ shows a metallicity gradient in very good agreement with data, but the value of $[\langle Mg/Fe\rangle]$ in the central region is -0.3, i.e. too low. In fact, the values suggested by population synthesis studies (Worthey et al. 1992; Weiss, Peletier & Matteucci 1995) indicate positive values for this ratio. This result is mainly caused by the late occurrence of galactic winds in the centre of the galaxy, which allows the supernovae of Type Ia to restore the bulk of iron before star formation stops. However, as discussed by Gibson (1997), yields different from those adopted here may increase the value of $[\langle Mg/Fe\rangle]$ but only on short time-scales, namely when the contribution of massive stars is still dominant. In fact, at late times, when the SNe Ia are appearing, the $[\langle Mg/Fe\rangle]$ ratio decreases because of the newly injected iron. In addition, this model predicts that $[\langle Mg/Fe\rangle]$ should increase with increasing radius, clearly at variance with what is inferred from metallicity indices. On the other hand, model B2 with $x = 0.95$ shows a metallicity gradient generally flatter than the observational data but a better ratio $[\langle Mg/Fe\rangle]$ ($+0.15$ in the central region). However, the best model seems to be model IV with a variable IMF, which shows a good metallicity gradient and a correct value of $[\langle Mg/Fe\rangle]$ in the centre and in the other galactic regions. This best model also predicts SN rates (expressed in units of SNu, namely SNe century^{-1} 10^{-10} $L_{B_\odot}$) and blue luminosity at the present time in good agreement with observations (Turatto, Cappellaro & Benetti 1994), namely the average supernova rates are $(R_{SNIa})_{R_e} = 0.11$ SNu, $(R_{SNII})_{R_e} = 0.02$ SNu. The predicted integrated blue luminosity for the whole galaxy, calculated as in Matteucci (1994), is $L_\odot = 7 \times 10^9$ $L_{B_\odot}$.

4 CONCLUSIONS AND DISCUSSION

In this paper we have explored the possibility of explaining metallicity gradients in giant ellipticals by means of models of chemical evolution including galactic winds. We have analysed the case of an elliptical galaxy with initial luminous mass $M_{lum} = 10^{11}$ $M_\odot$, $R_e = 3$ kpc and with a dark matter halo 10 times more massive than the luminous mass.

We found that, in order to reproduce most of the observational constraints relative to elliptical galaxies, the following constraints should hold.

(i) The dark matter should not be distributed like the luminous matter, but should be more diffuse. This result reinforces a previous analysis made by Matteucci (1992).

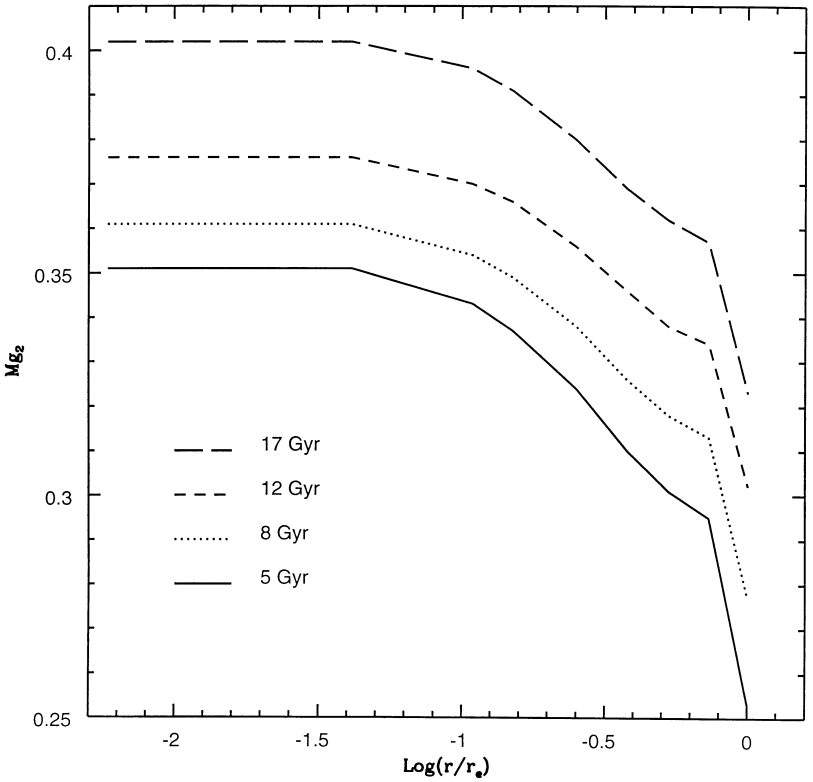

Figure 4. Gradients of the index Mg_2 as predicted by our model IV, using the calibrations of Worthey (1994) referring to different ages.

(ii) Abundance gradients in the stellar populations of ellipticals can be obtained by assuming that galactic winds develop first in the outer and later in the inner galactic regions, in agreement with the observational evidence of a correlation between the gas escape velocity and metallicity (Franx & Illingworth 1990; Davies et al. 1993; Carollo & Danziger 1994). The physical justification for this resides in the fact that the force required to carry out mass from the external regions is lower than that required to carry out mass in the internal regions. This mechanism for the formation of gradients is different from the mechanism often invoked (Larson 1974; Carlberg 1984; Greggio 1997). In this framework, an abundance gradient should arise because the stars form everywhere in collapsing clouds and then remain in orbit with a little inward motion whereas the gas sinks further in because there is dissipation. This gas contains the metals ejected by evolving stars so that an abundance gradient develops in the gas. As stars continue to form, their composition reflect the gaseous abundance gradient.

Our model does not exclude a mechanism of this type, which can be present together with the galactic winds occurring at different epochs in different regions. What we want to show here is that the differential occurrence of galactic winds alone can explain the observed abundance gradients. On the other hand, a mechanism of inside-out galaxy formation, such as that required to reproduce abundance gradients in the disc of our Galaxy (Matteucci & François 1989; Chiappini, Matteucci & Gratton 1997), does not seem to be suitable for elliptical galaxies. In fact, in order to reproduce the abundance gradient in the disc of our Galaxy one needs a large delay between the formation, caused by infall of gas, of the internal and the external parts of the disc, of the order of several billion years (Chiappini et al. 1997). This would imply that most ellipticals should be still forming now, with active star formation such as in the discs of spirals, at variance with observations. The advantage of the model proposed here over other models such as that of Larson (1974) is that it explains the observed correlation between colours/metallicity and escape velocity.

A final remark concerns the star formation efficiency, which we have assumed to be constant with galactocentric distance. We have also tried to vary this efficiency with galactocentric distance in the sense of having a higher efficiency in central regions. We found that for moderate variations of the efficiency of star formation the abundance gradients steepen together with the gradient in $[\langle \mathrm{Mg/Fe} \rangle]$. On the other hand, if the variation of ν is too strong the trend for the galactic wind is reversed, occurring later in the outermost regions with the consequence of cancelling the abundance gradients.

However, a potential problem with the mechanism for the formation of gradients suggested here is that it would predict an increasing $[\langle \mathrm{Mg/Fe} \rangle]$ as a function of the galactocentric distance, at variance with observations, unless a variable IMF is assumed at the same time.

In order to obtain an almost constant $[\langle \mathrm{Mg/Fe} \rangle]$ as a function of the galactocentric distance, as suggested by observations (Worthey et al. 1992; Carollo et al. 1993; Carollo & Danziger 1994), one has also to assume that the IMF varies with radius. In particular, x should vary from 0.95 at the galaxy centre up to 1.21 in the outermost regions. This would imply a slightly higher percentage of massive stars in the innermost regions, thus further favouring the abundance gradients. However, the observed trend of $[\langle \mathrm{Mg/Fe} \rangle]$ is inferred from the metallicity indices, which are also affected by other parameters such as age. Therefore, it is very important to have reliable $[\langle \mathrm{Mg/Fe} \rangle]$ ratios as a function of the galactocentric distances in ellipticals in order to assess this point.

The required IMF, in order to obtain positive values of $[\langle \mathrm{Mg/Fe} \rangle]$, especially in the galaxy centre, as suggested by the observations (Worthey et al. 1992; Weiss et al. 1995), must have a slope $x = 0.95$ in agreement with previous studies (MG; Gibson and Matteucci 1997), although a variation in the stellar yields could achieve the same result (Gibson 1997), but only if the time-scale for the galactic wind is short enough (Weiss et al. 1995).

Another potential problem could be the fact that in our best model (model IV) the galactic wind does not develop until 12 Gyr in the most internal regions (< 150 pc). However, it should be noted that, because of the fast consumption of gas, star formation occurs at such a low level at 12 Gyr that the Type II SNe would be scarcely detectable.

Finally, we want to discuss the consequences of our model on the chemical evolution of the intracluster medium, although more details will be found in a future paper. The late occurrence of galactic winds in the more internal regions of ellipticals, if true, will have as a consequence a continuous chemical evolution of the ICM, at variance with the predictions made by models with only early winds (MG; Gibson and Matteucci 1997), which predict no evolution of the ICM starting from very high redshift ($z \leq 4$–5). This prediction can be checked in future with observations of abundances in high-redshift clusters; preliminary results from *ASCA* (Mushotsky and Lowenstein 1997) seem to indicate no evolution in the abundance of Fe for $z < 0.3$.

REFERENCES

Angeletti L., Giannone P., 1990, A&A, 234, 53
Arimoto N., Yoshii Y., 1986, A&A, 164, 260
Arimoto N., Yoshii Y., 1987, A&A, 173, 23
Barbuy B., 1994, ApJ, 430, 218
Bender R., Burstein D., Faber S. M., 1992, ApJ, 399, 462
Bender R., Burstein D., Faber S. M., 1993, ApJ, 411, 153
Bertin G., Saglia R. P., Stiavelli M., 1992, ApJ, 384, 423
Bressan A., Chiosi C., Fagotto F., 1994, ApJS, 94, 63
Brocato E., Matteucci F., Mazzitelli I., Tornambè A., 1990, ApJ, 349, 458
Burnstein D., Faber S. M., Gaskell C. M., Krumn N., 1984, ApJ, 287, 586
Buzzoni A., Gariboldi G., Mantegazza L., 1992, AJ, 103, 1814
Canizares C. R., Fabbiano G., Trinchieri G., 1987, ApJ, 312, 503
Carlberg R., 1984, ApJ, 286, 404
Carollo C. M., Danziger I. J., 1994, MNRAS, 270, 523
Carollo C. M., Danziger I. J., Buson L., 1993, MNRAS, 265, 553
Chiappini C., Matteucci F., Gratton R., 1997, ApJ, 477, 765
Cioffi D. F., McKee C. F., Bertschinger F., 1988, ApJ, 334, 252
Cox D. P., 1972, ApJ, 178, 159
Davies R. L., Sadler E. M., Peletier R. F., 1993, MNRAS, 262, 650
Dressler A., Lynden-Bell D., Burnstein D., Davies R. L., Faber S. M., Terlevich R. J., Wegner G., 1987, ApJ, 313, 42
Faber S. M., 1972, A&A, 20, 361
Faber S. M., 1977, in Tinsley B. M., Larson R. B., eds, Evolution of Galaxies and Stellar Populations. Yale University Observatory, New Haven, p. 157
Faber S. M., Jackson R. E., 1976, ApJ, 204, 668
Faber S. M., Friel E. D., Burnstein D., Gaskell C. M., 1985, ApJS, 57, 711
Ferrini F., Poggianti B. M., 1993, ApJ, 410, 44
Forman W., Jones C., Tucker W., 1985, ApJ, 293, 102
Franx M., Illingworth G., 1990, ApJ, 359, L41
Gibson B. K., 1994, MNRAS, 271, L35
Gibson B. K., 1997, MNRAS, 290, 471
Gibson B. K., Matteucci F., 1997, ApJ, 457, 47

Greggio L., 1997, MNRAS, 285, 151
Jaffe W., 1983, MNRAS, 202, 995
Kauffmann G., 1996, MNRAS, 281, 487
Kauffmann G., Charlot S., 1998, MNRAS, 294, 705
Kormendy J., Djorgovski S., 1989, ARA&A, 27, 235
Larson R. B., 1974, MNRAS, 166, 585
Mathews W. G., Baker J. C., 1971, ApJ, 170, 241
Matteucci F., 1992, ApJ, 397, 32
Matteucci F., 1994, A&A, 288, 57
Matteucci F., François P., 1989, MNRAS, 239, 886
Matteucci F., Gibson B., 1995, A&A, 304, 11 (MG)
Matteucci F., Greggio L., 1986, A&A, 154, 279
Matteucci F., Padovani P., 1993, ApJ, 419, 485
Matteucci F., Tornambè A., 1987, A&A, 185, 51
Michard R., 1983, A&A, 121, 313
Mould J. R., 1978, ApJ, 220, 434
Mushotsky R. F., Lowenstein M., 1997, ApJ, 481, L63
Pagel B. E. J., Patchett B. E., 1975, MNRAS, 172, 13
Peletier R. F., 1989, PhD thesis, Univ. Groningen
Prochaska J. X., Wolfe A. M., 1997, ApJ, 487, 73
Renzini A., 1995, in van der Kruit P. C., Gilmore G., eds, IAU Symp. 164, Stellar Populations. Reidel, Dordrecht, p. 325
Renzini A., Ciotti L., 1993, ApJ, 416, L49
Renzini A., Voli M., 1981, A&A, 94, 175
Salpeter E. E., 1955, ApJ, 121, 161
Tantalo R., Bressan A., Chiosi C., 1998, A&A, 333, 419
Thielemann F. K., Nomoto K., Hashimoto M., 1993, in Prantzos N., Vanpiori-Flam E., Cassé M., eds, Origin and Evolution of the Elements. Cambridge Univ. Press, Cambridge, p. 297
Turatto M., Cappellaro E., Benetti S., 1994, AJ, 108, 202
van den Marel R. P., 1991, MNRAS, 253, 710
Weiss A., Peletier R., Matteucci F., 1995, A&A, 296, 73
Woosley S. E., 1987, in Hauck B., Maedev A., Meynet G., eds, 16th Saas Fee Course, Nucleosynthesis and Chemical Evolution. Geneva Observatory, Geneva, p. 1
Worthey G., 1994, ApJS, 95, 107
Worthey G., Faber S. M., Gonzalez J. J., 1992, ApJ, 398, 73
Zepf S. E., Silk J., 1996, ApJ, 466, 114
Ziegler B. L., 1997, in da Costa L., Renzini A., eds, ESO Workshop, Galaxy Scaling Relations: Origin, Evolution and Applications, p. 209